Int. J. Heat Mass Transfer. Vol. 21, pp. 1385–1392

0017-9310/78/1101-1385 $02.00/0

MEASUREMENTS OF BOILING CURVES OF SUBCOOLED WATER UNDER FORCED CONVECTIVE CONDITIONS

S. C. CHENG, W. W. L. NG and K. T. HENG
Department of Mechanical Engineering, University of Ottawa, Ottawa, Canada

(*Received* 9 *February* 1978 *and in revised form* 10 *April* 1978)

Abstract—A high thermal capacity test section has been used to obtain boiling curves for distilled water at atmospheric conditions. The results obtained during transient conditions agreed with the steady state ones. The parametric effects of mass flux (range 68–203 kg/m²s) and subcooling (range 0–28°C) are discussed. The measured boiling curves have been compared with those available from the literature. It is concluded that most existing correlations cannot be relied upon to predict boiling heat transfer obtained under the present conditions.

NOMENCLATURE

C_p, specific heat;
CHF, critical heat flux;
D, diameter;
G, mass flux;
g, gravitational constant;
h, heat-transfer coefficient;
i_{fg}, latent heat of vaporization;
k, thermal conductivity;
p, pressure;
T, temperature;
t, time;
T.C., thermocouple;
x, quality.

Greek symbols
ΔT, temperature difference;
Δt, time interval;
μ, viscosity;
ρ, density;
σ, surface tension;
ϕ, heat flux.

Subscripts
e, equilibrium;
l, liquid;
sat, saturated;
sub, subcooled;
v, vapor;
w, wall.

INTRODUCTION

ALTHOUGH reactors normally operate at power levels well below the critical power, accidents can be postulated where the critical power is exceeded. In the thermal analysis of such postulated accidents it must be assumed that, when the critical heat flux is exceeded, the heat-transfer mode will change from the very efficient nucleate boiling mode to the less efficient transition boiling mode. At higher wall superheats, the transition boiling mode will change gradually to the inefficient flow film boiling mode. Conversely, in analysing the thermal behaviour of a hot surface which is being rewetted (such as may occur during emergency core cooling at a nuclear reactor) it must be assumed that flow film boiling is followed by transition boiling before nucleate boiling can be re-established.

Earlier version of present thermohydraulic codes frequently ignored the existence of a transition boiling mode; this resulted in an over prediction of the calculated sheath temperature history. Most present thermohydraulic codes include a transition boiling term. However, because of the scarcity of relevent data, transition boiling correlations have only a limited range of applicability and must be suspected because of their unreliable data base.

Forced convective transition boiling has been investigated by few investigators who have used both steady state and transient methods [1]. Systems used in these studies can either be heat flux controlled (electrical or nuclear heating, no thermal inertia), temperature controlled or a combination of both. During fast transient situation, most systems approach the behaviour of a temperature controlled system while during steady state situation or slow transients, nuclear fuel elements behave like a heat flux controlled system.

In this investigation, a cylindrical copper block was employed as the test section. The experimental data were obtained both during steady state and transient conditions. During steady state operation, the heat flux to the fluid was obtained from the power input to the heaters (after correcting for heat losses). The high thermal capacity of the block increases the transition boiling time during transient tests, thus permitting frequent and accurate measurement of transition boiling temperatures and heat flux values. The measuring technique used in this investigation permits the construction of complete boiling curves under forced convective conditions over a wide range of mass flows and subcoolings.

EXPERIMENTAL APPARATUS

The experimental apparatus consists primarily of a hot water storage tank, a flow meter, a pump and a test

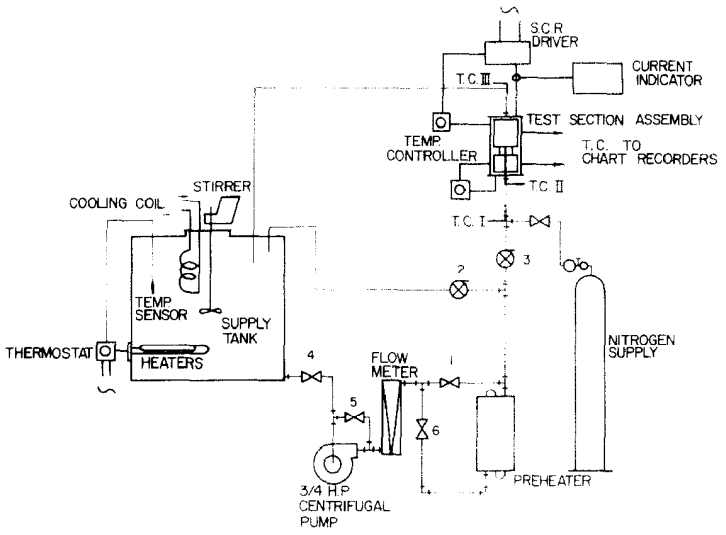

FIG. 1. Schematic diagram for the experimental loop.

section assembly as shown in Fig. 1. Provisions of bypassing the pump and the test section assembly were incorporated to stabilize the flow. The flow rate was measured by a rotometer and the flow adjustment was done via the flow control valve 1. Valves 2 and 3 are ON–OFF valves which operate out-of-phase, i.e. valve 2 open and valve 3 closed or vice versa. Thermocouples I, II and III were installed to measure temperatures of the flow, the inlet, and the outlet of the entrance heater and the exit temperature of the test section, respectively.

Test section assembly

The test section assembly as shown in Fig. 2, consists of a long copper block test section and a short copper block which acts as an entrance heater to establish the correct flow conditions and minimize heat losses. The

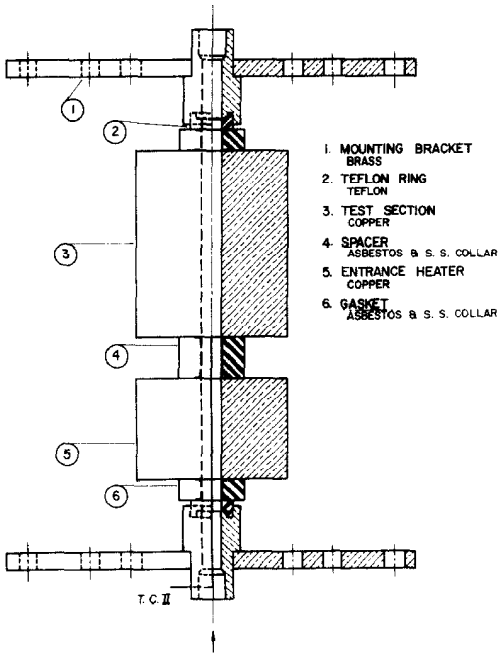

FIG. 2. Test section assembly.

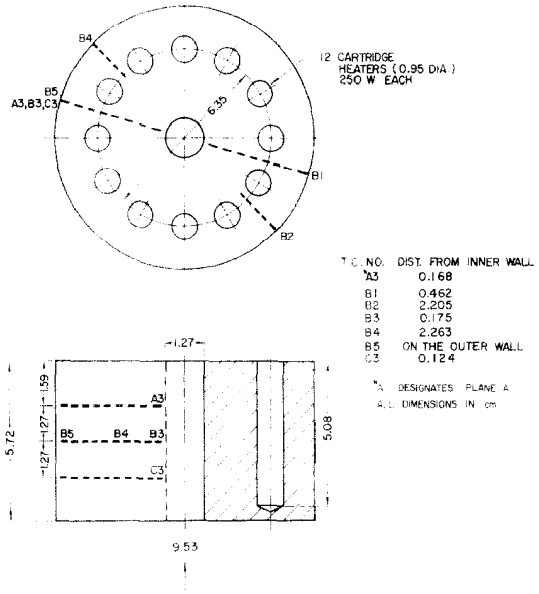

FIG. 3. Short block test section or entrance heater.

short copper block, which can also be used as a separate test section, consists of a 5.72 cm long copper cylinder with a 9.53 cm O.D. and a 1.27 cm dia central flow channel as shown in Fig. 3. The location of the seven chromel–alumel thermocouples and the twelve cartridge heaters is also shown. T.C.s A3, B3 and C3 were used for data thermocouples. The thermocouples were sheathed (by stainless steel wire with 0.1016 cm O.D.) and grounded. The sheathed thermocouples were press fitted into individual thermocouple holes and then silver soldered onto the outside test section surface. The structure of the long copper block test section is similar to the short copper block as illustrated in Fig. 4; where T.C.s A1, B1 and C1 were used for data thermocouples. Axial heat losses of the test section assembly were reduced by using asbestos gasket and asbestos spacer at the inlet and outlet of the two blocks as shown in Fig. 2. Circumfer-

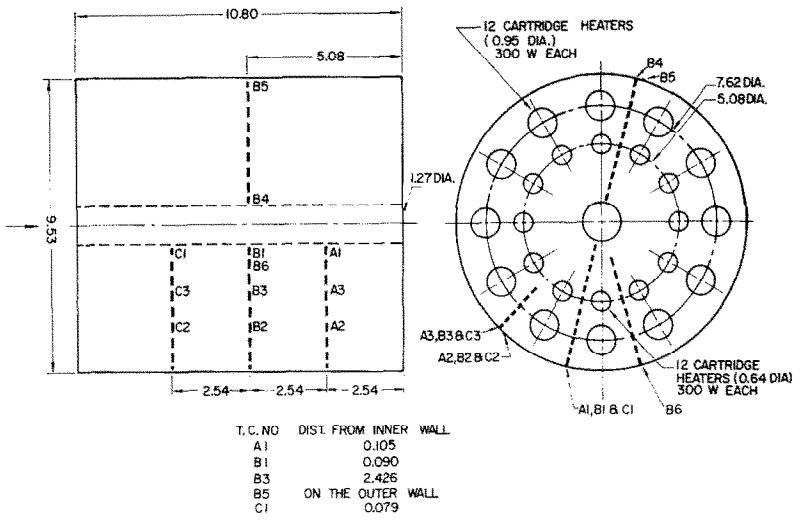

FIG. 4. Long block test section.

ential heat losses of the test section assembly were minimized by lagging the two blocks with a 5 cm thick ceramic fiber insulation.

Temperature controllers

Two types of temperature controllers were used, i.e. an ON–OFF temperature controller (Model R7353, Honeywell) and a proportional temperature controller (Model R7355, Honeywell). In general, the proportional temperature controller was employed to control the test section temperature during a steady state operation. The operation of the proportional controller was regulated by the Silicon Controlled Rectifier driver stage (Model LZF1, SCR Driver, HALMAR). This driver is of the zero firing type which only conducts current through the rectifier every 1/120 s. Within a fixed time interval, which is invariant for different makes and is determined by the manufacturer, the number of triggering pulses are proportional to the input signal of the temperature controller. In other words, the number of conducting cycles are directly proportional to the deviation between the set-point temperature and the controlling temperature (through T.C. B4 of Fig. 3 or T.C. B3 of Fig. 4).

Further details of the experimental apparatus, and the method of controlling temperature and measuring power are given in [2].

EXPERIMENTAL PROCEDURES

The following procedures were followed for obtaining experimental data during transient conditions.

(i) Water in the storage tank was first heated to the desired coolant temperature using immersion heaters which were thermostatically controlled.

(ii) The loop circulation pump was then switched on and the flow was passed first through flow control valve 1, then through ON–OFF valve 2 (valve 3 closed) and was drained back to the storage tank via the test section by-pass loop.

(iii) The test section and the entrance heater were heated up to the required initial temperatures. During the heating up period, nitrogen was circulating through the test section assembly to prevent oxidation at high heated surface temperatures.

(iv) At the start of the transient test run, nitrogen supply was stopped and the test section power was turned off, then valve 2 was closed and valve 3 was opened to divert the flow through the test section.

(v) The temperature of the entrance heater was maintained constant by the temperature controller throughout a given run. Chart recorders and data acquisition system were started as soon as test section inlet conditions were established.

The experimental procedures for the steady state method are very similar to those of the transient method except the following:

(i) Temperature of the test section (T.C. B1, Fig. 4) was initially set well into the film boiling region and was maintained at that level by the temperature controller during each experimental run.

(ii) The experiment was repeated at lower heated surface temperatures until a complete boiling curve was obtained.

The heat-transfer coefficient at the outer wall for the two copper blocks is required for heat flux calculations for both transient and steady state methods. It has been determined experimentally at approximately 17 W/m^2 °C under a no-flow condition.

EXPERIMENTAL RESULTS

Two series of experiments were conducted; the first series (Run numbers 500–599) utilized the short block as the test section while the long block remained unheated, whereas the second series (Run numbers 400–499) used the long block as the test section with the short block as the entrance heater.

Short block series

The experimental procedures for this series are similar to those described in the previous section.

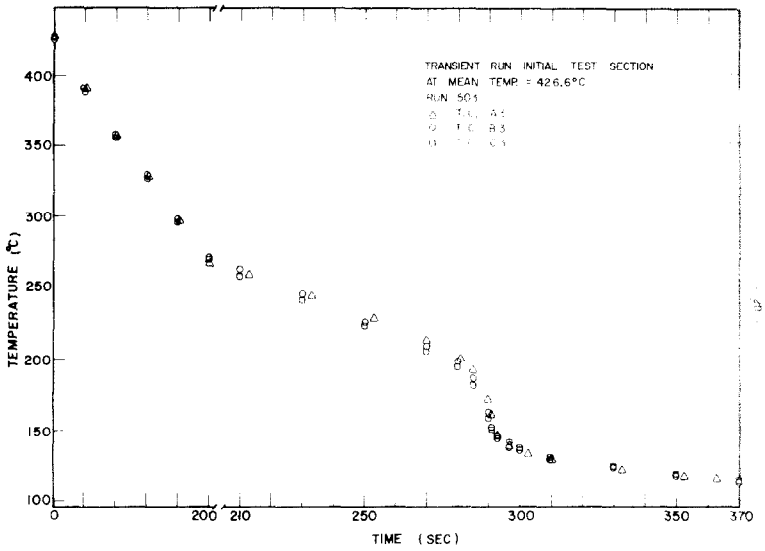

FIG. 5. Temperature traces, short block series for $G = 136\,\text{kg/m}^2\text{s}$ and $\Delta T_{sub} = 13.9°\text{C}$.

Figure 5 shows some typical temperature traces based on T.C.s A3, B3 and C3 for a mass flux of $136\,\text{kg/m}^2\text{s}$ and a subcooling of 13.9°C. From the temperature traces, it appears that axial conduction is insignificant. Boiling curves based on Fig. 5 thermocouple traces were constructed using the technique developed in reference [3, 4] and are presented in Fig. 6. Basically, the technique allows one to calculate heat flux from the test section to the fluid between time t to $t+\Delta t$ by computing the change in stored heat in the test section, minus heat losses through outside wall during the time interval Δt.

In the data reduction, it was assumed that the heaters presence did not affect the temperature transients. This is justified since (a) the volumetric heat capacity (ρC_p) of the heaters is similar to that of copper, (b) the heaters only occupy a portion of the test section volume and (c) the heaters are distributed evenly around the periphery of the test section and do not introduce a non-uniform circumferential temperature distribution at the inside heated surface. During the steady state runs, the heat flux to the fluid was obtained directly from the power input to the heaters after correction for heat losses.

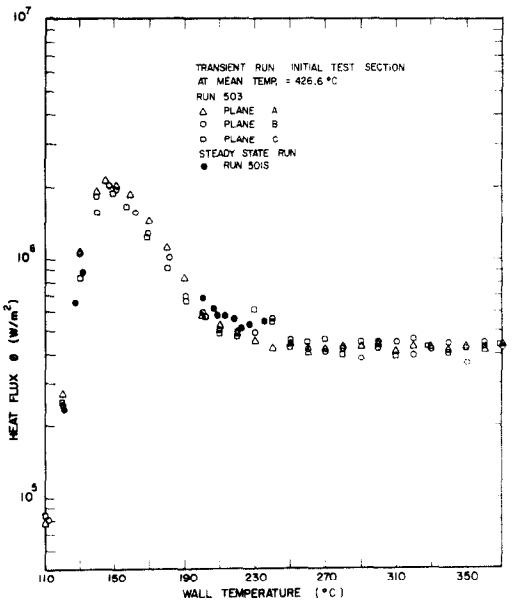

FIG. 6. Boiling curves of distilled water, short block series for $G = 136\,\text{kg/m}^2\text{s}$ and $\Delta T_{sub} = 13.9°\text{C}$.

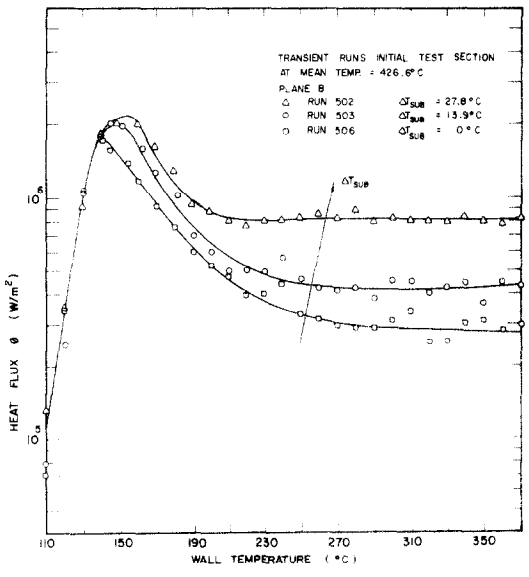

FIG. 7. Effect of subcooling on boiling curves of distilled water, short block series for $G = 136\,\text{kg/m}^2\text{s}$.

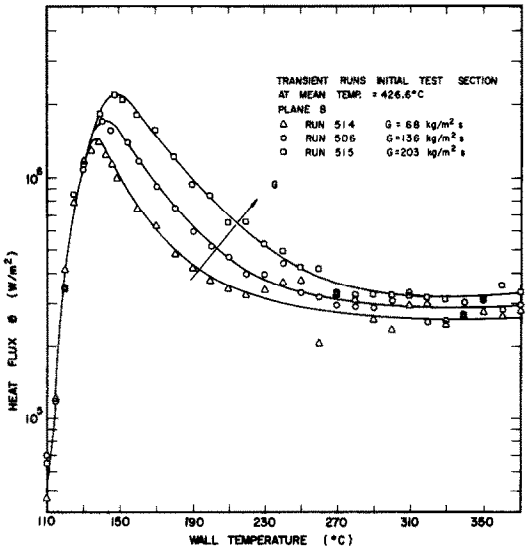

FIG. 8. Effect of mass flux on boiling curves of distilled water, short block series for $\Delta T_{sub} = 0°C$.

Figure 7 illustrates the effect of inlet subcooling on the boiling curves for a mass flux of 136 kg/m²s, while the effect of mass flux for a subcooling of 0°C is shown in Fig. 8.

Long block series

The purpose of using the entrance heater in this series is to generate a two-phase subcooled fluid at the inlet of the test section, and to further minimize axial heat losses of the test section. Figure 9 presents some typical boiling curves based on T.C.s A1, B1 and C1 for a mass flux of 136 kg/m²s and a subcooling of 5.6°C with the entrance heater set at constant temperature of 315.5°C. Notice that the degree of subcooling in this series represents an equilibirum two-phase fluid temperature at the outlet of the entrance heater or the inlet of the test section. It can be determined by the following two techniques (the presence of non-equilibrium does not permit a direct measurement of coolant temperature).

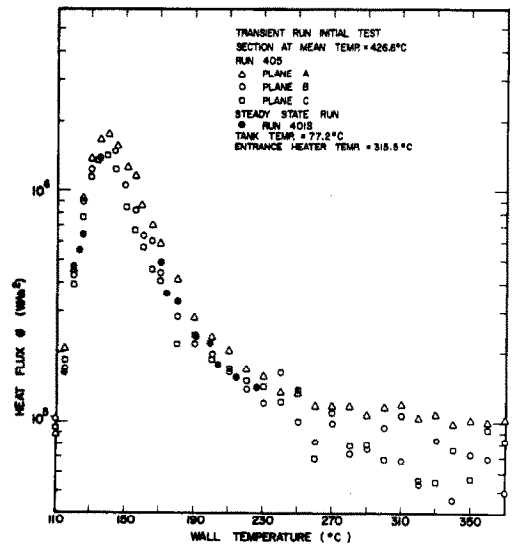

FIG. 9. Boiling curves of distilled water, long block series for $G = 136 kg/m^2s$ and $\Delta T_{sub} = 5.6°C$.

The first technique evaluates the coolant enthalpy rise in the entrance heater from the flow and entrance heater power measurement. The second technique evaluates the entrance heater power from the boiling heat flux measured under identical flow conditions in the short block series. It then evaluates the enthalpy size in the entrance heater as done in the first technique. Both techniques yield close results, however, due to simplicity, the second method is chosen.

The temperature of the entrance heater was set well into the film boiling regime in a given run to allow stable film boiling established inside the entrance heater with subcooled liquid passing through. However, when the liquid at moderate inlet temperatures passed through the entrance heater, the exit flow was invariably close to saturation temperature. If the inlet liquid temperature decreases, then quenching occurs inside the entrance heater, thus no stable film boiling can be maintained. As a result, in the long block series, only a small range of subcooling (at the inlet of the test section) exists, e.g. less than 6°C for a mass flux of 136 kg/m²s. The experimental results from this series indicate a similar trend on the effects of subcooling and mass flux on boiling curves as the trend displayed by the short block series.

DISCUSSION

Newbold's [5] and Fung's [6] experimental data suggest that the film boiling portion of the boiling curve is almost independent of wall superheat. Figures 6–8 show that present experimental results display a similar trend. Some fluctuation in surface temperature and heat flux was observed at lower subcooling runs, e.g. Run 506 in Fig. 7. This is thought to be due to the presence of slug flow. A subsequent study by Ragheb [7] using a transparent section near the test section showed that slug formation occurred during transition boiling. The associated variation in the heat-transfer coefficient could have resulted in the observed fluctuation in surface temperature.

During some of the runs, steady state data were obtained in addition to the transient results. Figures 6 and 9 show that the difference between the steady state and transient results is negligible. This was expected as the high thermal capacity of test section slowed down the quenching process to make the system act in a pseudo-steady-state manner.

A comparison with data and correlations from other sources is shown in Figs 10–12. Figure 10 shows a comparison with Fung's nucleate boiling results obtained in a similar test section. As can be seen, the data sets are in good agreement. However, a comparison with Jens–Lottes' correlation [8] (all the correlations employed in this study are presented in Table 1), and Thom's correlation [9] show that both correlations

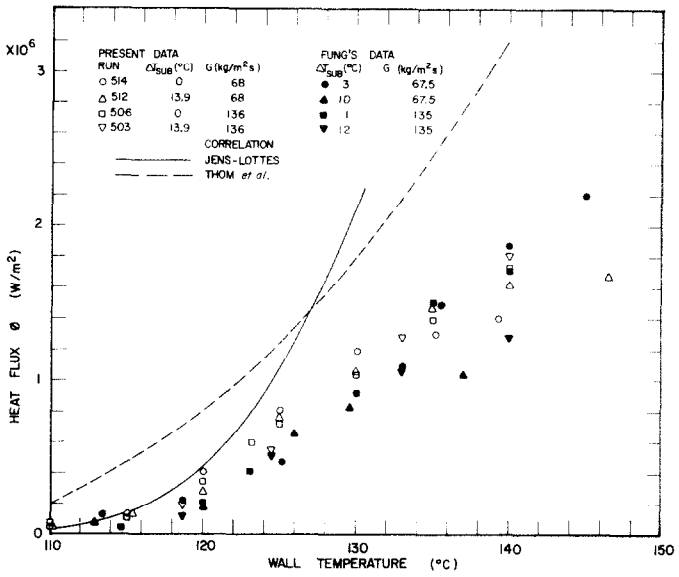

FIG. 10. Comparison of data in the nucleate boiling regime.

overpredict the experimental data at higher wall superheats.

Figure 11 presents an example of present data and Fung's transition boiling results. It was found that, for the mass flux range and subcooling range studied, relations only predict a general trend of the boiling curve and do not show an effect of subcooling.

In the film boiling regime, Groeneveld and Gardiner's data [13] are superimposed with present data as illustrated in Fig. 12. It is noticed that the

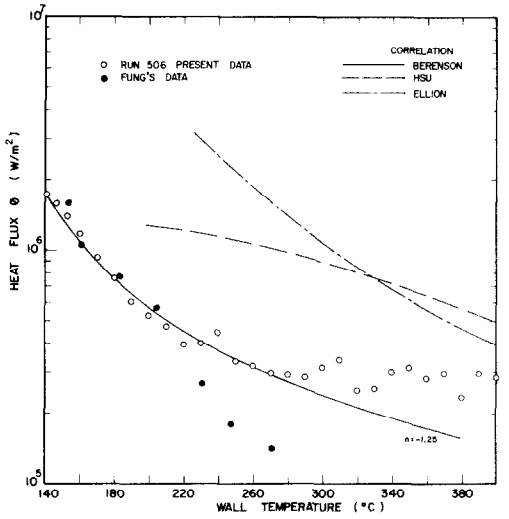

FIG. 11. Comparison of data in the transition boiling regime, short block series for $G = 136\,\text{kg/m}^2\,\text{s}$ and $\Delta T_{sub} = 0°\text{C}$.

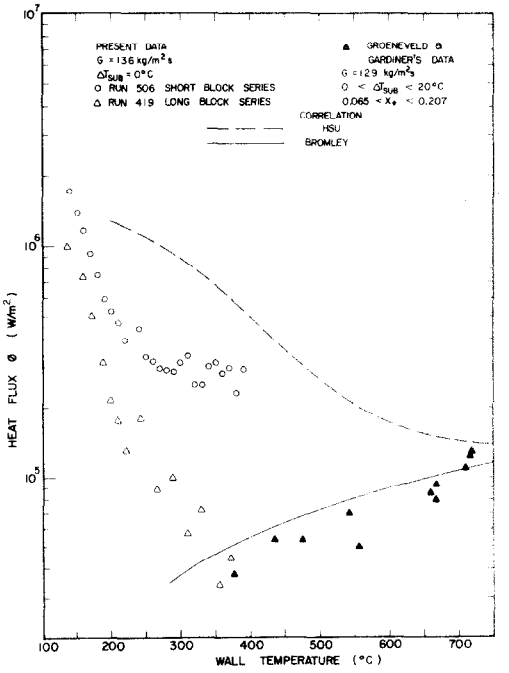

FIG. 12. Comparison of data in the film boiling regime.

Berenson's type transition boiling correlation [10] having the form

$$\frac{\phi}{\text{CHF}} = \left(\frac{\Delta T_{sat}}{T_{CHF} - T_{sat}}\right)^{-1.25}$$

agreed with present data. The limitations of Berenson's correlation are that both CHF and T_{CHF} have to be known beforehand. Other correlations, such as Hsu's transition and film boiling correlation [11] and Ellion's transition boiling correlation [12] are also shown for comparison. Both Hsu's and Ellion's correlations

present data from the long block series match nicely with their data. This is thought to be due to the fact that the local quality at the data thermocouple T.C. B1 is close to the local quality of their data thermocouple. Hsu's correlation and Bromley's film boiling correlation [14, 15] are also presented in Fig. 12. Bromley's correlation yields a good trend over present data and those of Groeneveld and Gardiner.

Table 1. Boiling heat-transfer correlations

Jens–Lottes [8]	$\Delta T_{sat} = 25\,\phi^{0.25}\,e^{-p/62}$
Thom [9]	$\Delta T_{sat} = 22.65\,\phi^{0.5}\,e^{-p/87}$
Hsu [11]	$h = 0.62\left\{\dfrac{k_v^3\,\rho_v(\rho_l-\rho_v)\,g\,i'_{fg}}{\mu_v\Delta T_{sat}(2\pi)\left[\dfrac{\sigma}{g(\rho_l-\rho_v)}\right]^{1/2}}\right\}^{1/4} + A\exp(-B\Delta T_{sat})$
	$A = 1456\,p^{0.558}$
	$B = 3.758\times10^{-3}\,p^{0.1733}$
Ellion [12]	$\phi = 4.562\times10^{11}\times\Delta T_{sat}^{-2.4}$
Bromley [14, 15]	$h = 0.62\left[\dfrac{k_v^3\,g\,\rho_v(\rho_l-\rho_v)\,i'_{fg}}{D\,\mu_v\Delta T_{sat}}\right]^{1/4}$
	$i'_{fg} = i_{fg}\left(1+\dfrac{0.4\,C_p\Delta T_{sat}}{i_{fg}}\right)^2$

In general, measurements on the long block series produce lower post-CHF heat flux values than measurements on the short block series. Particularly, the long block series heat flux during the initial stage of transient run (film boiling regime) is much lower as shown in Fig. 12. This is thought to be due to the presence of non-equilibrium during the long block series, where the vapor film was established in the entrance heater and can be considerably thicker than in the short block series where the vapor film becomes established near the entrance of the test section. The thicker vapor film is thought to present a considerable resistance to heat transfer thus lowering the film boiling heat flux for the same equilibrium conditions compared to the short block series.

A study on the effect of heated surface thermal properties on boiling curves is in progress. Preliminary results from a composite test section constructed of Inconel tubing soldering inside a copper block indicates that the values of CHF and minimum heat flux show little change, but the rewetting occurs at approximately 50–60°C higher wall superheat.

CONCLUSIONS

1. The boiling curves obtained via both transient and steady state methods, in general, are in good agreement. Transition boiling heat flux increases with increasing subcooling and mass flux within the range of the flow parameters investigated (mass flux range 68–203 kg/m^{2}s and subcooling range 0–28°C). Present transition boiling correlations do not display such an effect and should, therefore, be suspected.

2. The experimental data show no effect of subcooling and mass flux on the nucleate boiling curves (Fig. 10). This is in agreement with the data and correlations of Thom, and Jens and Lottes.

3. Based on the results of short block series, the heat flux in the film boiling regime remains constant over a fairly wide range of wall superheats.

4. Most existing correlations overpredict boiling heat transfer obtained under the present conditions and should, therefore, be suspected.

Acknowledgements—The authors wish to express their gratitude to the U.S. Nuclear Regulatory Commission for providing the financial support for this project. The authors also extend their thanks to Dr. D. C. Groeneveld for his many valuable suggestions throughout the course of study.

REFERENCES

1. D. C. Groeneveld and K. K. Fung, Forced convective transition boiling review of literature and comparison of prediction methods AECL-5543 (June 1976).
2. S. C. Cheng, W. W. L. Ng, K. T. Heng and H. Ragheb, Transition boiling heat transfer in forced vertical flow, Final Report, for the period June 1976–June 1977, Argonne Contract No. 31-109-38-3564 (June 1977).
3. S. C. Cheng and K. T. Heng, A technique to construct a boiling curve from quenching data, the *Letters Heat Mass Transfer* 3, 413–420 (1976).
4. S. C. Cheng, K. T. Heng and W. Ng, A technique to construct a boiling curve from quenching data considering heat loss, *Int. J. Multiphase Flow* 3, 495–499 (1977).
5. F. J. Newbold, J. C. Ralph and J. A. Ward, Post-dryout heat transfer under low flow and low quality conditions, AERE-R8390 (1976).
6. K. K. Fung, Forced convective transition boiling, M.A.Sc. Thesis, Dept. of Mechanical Engineering, Univ. of Toronto (1976).
7. H. Ragheb, Development of probe to detect phase change at a heated surface, M.A.Sc. Thesis, Dept. of Mechanical Engineering, Univ. of Ottowa (December 1977).
8. W. H. Jens and P. A. Lottes, Analysis of heat transfer burnout, pressure drop and density data for high pressure water, ANL-4627 (May 1951).
9. J. R. S. Thom, W. M. Walker, T. A. Fallon and G. F. S. Reising, Boiling in subcooled water during flow up heated tubes or annuli, Paper 6 presented at the *Symposium on Boiling Heat Transfer in Steam Generating Units and Heat Exchangers*, Manchester (September 1965).
10. P. J. Berenson, Transition boiling heat transfer from a horizontal surface, MIT Technical Report No. 17 (1960).
11. Y. Y. Hsu, Tentative correlation of reflood heat transfer, presented at the Third Water Reactor Safety Information Meeting, Germantown, Maryland (1975).

12. M. E. Ellion, A study of the mechanism of boiling heat transfer, California Inst. of Technology report, JPL-MEMO-20-88 (1954).
13. D. C. Groeneveld and S. R. M. Gardiner, A method of obtaining flow film boiling data for subcooled water, *Int. J. Heat Mass Transfer* **21**, 664–665 (1978).
14. L. A. Bromley, Heat transfer in stable film boiling, *Chem. Engng Prog.* **46**, 221–227 (1950).
15. L. A. Bromley, N. R. LeRoy and J. A. Robbers, Heat transfer in forced convection film boiling, *Ind. Engng Chem.* **45**, 2639–2646 (1953).

DETERMINATION DES COURBES D'EBULLITION D'EAU SOUS-REFROIDIE DANS DES CONDITIONS DE CONVECTION FORCEE

Résumé—On utilise une section d'essai à grande capacité thermique pour obtenir des courbes d'ébullition d'eau distillée à pression atmosphérique. Les résultats obtenus durant le régime transitoire s'accordent avec ceux du régime permanent. On discute les effets du flux massique (variable de 68 à 203 kg/m^{2}s) et du sous-refroidissement (de 0° à 28°C). Les courbes d'ébullition obtenues sont comparées avec celles disponibles dans la bibliographie. On conclut que la plupart des formules existantes ne peuvent être appliquées au transfert thermique par ébullition obtenu dans les conditions de cette étude.

BESTIMMUNG DER SIEDEKURVEN VON UNTERKÜHLTEM WASSER BEI ERZWUNGENER KONVEKTION

Zusammenfassung—Zur Bestimmung der Siedekurven von destilliertem Wasser bei atmosphärischen Bedingungen wurde eine Meßstrecke mit hoher Wärmekapazität benutzt. Die Ergebnisse, die bei instationären Bedingungen gewonnen wurden, stimmen mit den Ergebnissen überein, die im stationären Zustand gewonnen wurden. Die Einflüsse der Massenstromdichte (Bereich 68 ... 203 kg/m^{2}s) und der Unterkühlung (Bereich 0 ... 28°C) werden diskutiert. Die gemessenen Siedekurven wurden mit in der Literatur vorhandenen verglichen. Man kann daraus folgern, daß bei der Berechnung des Wärmeüberganges beim Sieden unter den genannten Bedingungen den meisten vorhandenen Korrelationen nicht vertraut werden kann.

КРИВЫЕ КИПЕНИЯ НЕДОГРЕТОЙ ВОДЫ В УСЛОВИЯХ ВЫНУЖДЕННОЙ КОНВЕКЦИИ

Аннотация — Для определения кривых кипения дистиллированной воды при атмосферных условиях использовался рабочий участок с большой теплоёмкостью. Результаты, полученные при нестационарных условиях, находятся в хорошем согласии с результатами для стационарного случая. Рассматривалось влияние теплового потока (в диапазоне от 68 до 203 кг/м^{2}с) и недогрева (в диапазоне от 0 до 28°C). Измеренные кривые кипения сравнивались с кривыми, известными из литературы. Сделан вывод о том, что большинство из существующих соотношений не могут использоваться для расчёта теплообмена при кипении в данных условиях.